# Mutual injection locking of oscillator circuits through inductor coupling

A. Suárez[1], F. Ramírez[1], R. Melville[2]
[1]DICOM, University of Cantabria, Spain
[2]EMECON LLC, USA

***Abstract*—This work presents an investigation of mutual injection locking of oscillator circuits through inductor coupling. A realistic analytical formulation provides insight into system behavior, with coexistent oscillation modes. The stability of these modes is determined through a perturbation analysis, extended to the calculation of the phase-noise spectral density. An analytical expression enables an understanding of the phase-noise reduction mechanism. The cases of two coupled oscillators at the fundamental frequency and two distinct oscillators at a 1/3 frequency ratio are considered. Possible applications include the oscillator phase-noise reduction and the implementation of sensors using the phase shift between the two oscillator elements.**

***Keywords*—oscillators, harmonic balance, stability analysis, phase-noise analysis.**

## I. Introduction

Recently, successful implementations of multi-core oscillator circuits based on inductive coupling have been demonstrated [1]-[3]. The coupling effects enable a phase-noise reduction as $S_N = S - 10\log_{10}N$, where $S$ is the spectral density of a single oscillator and $N$ is the number of oscillator elements. However, two problems are pointed out: the coexistence of oscillation modes and the undesired impact of the oscillator asymmetries. Other possible applications include sensors [4] and near-field wireless data systems, in the vein of one described in [5] at 13.35 MHz and 30 MHz. Despite the interest of inductive coupling, there is a lack of practical and insightful analysis tools. The work [3] proposes a useful eigenvector/eigenvalue analysis [6] of the full oscillator system, which takes advantage of the circular symmetry of the coupling matrix. The coexistent oscillation modes are identified, but no stability analysis is carried out. Furthermore, the analysis will not be valid in the presence of asymmetries.

This work presents an investigation of two mutually injection-locked oscillators through inductor coupling (Fig. 1). It is based on the use of realistic models of the individual oscillators, extracted from harmonic-balance (HB) simulations [7]. The stability analysis will avoid the uncertainty of the oscillation mode that will be observed experimentally. In comparison with previous approaches [1], the derived phase-noise analysis will be general and realistic, and will enable a prediction of the impact of the original oscillator design and the inductive coupling. Two cases are considered. The first one [Fig. 1(a)] consists of two simple Van der Pol oscillators coupled at the fundamental frequency. This will enable a detailed validation of the analysis method through a comparison with circuit-level HB simulations, which fail to converge in more complex practical circuits. The second case [Fig. 1(b)] will be that of two different oscillators that under the inductive coupling effects are able to synchronize at the frequency ratio 1/3. The oscillators with a cross-coupled topology have been manufactured and measured. The main inductive coupling mechanism occurs between the third harmonic component of the oscillator at the lower frequency $\omega_1$ and the fundamental frequency of the second oscillator at $\omega_3$, which provides the relationship $\omega_3 = 3\omega_1$. In addition to phase-noise reduction, we propose two possible applications, derived from the rather large sensitivity of phase shift between the oscillators to a variation of the capacitor or inductor of the oscillator at $\omega_1$. A specific measurement technique for this phase shift has been implemented. The work [4] considers a sensing application in which a sample responds more to the magnetic field at $\omega_1$ than to the field at $\omega_3$. Hence, introducing a signal into the coupled magnetic field will cause a detectable phase shift. Another possible application would be a mechanical sensor that changes either the capacitor or inductor of the $\omega_1$ oscillator [4].

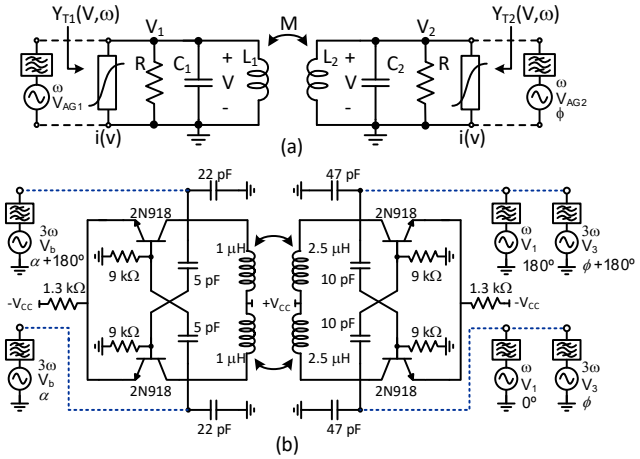


Fig. 1. Inductively coupled oscillators. AGs are used to extract the oscillator models. (a) Simple circuit used for the analysis validation through comparison with HB simulations. (b) Practical coupled circuit at the frequency ratio 1/3.

## II. Coupling at the Fundamental Frequency

### A. Steady state

The system of two oscillators coupled through their inductors is shown in Fig. 1(a). The admittance matrix that models the two coupled inductors (assumed ideal) is purely imaginary and given by:

$$\begin{bmatrix} y_{11} & y_{12} \\ y_{21} & y_{22} \end{bmatrix} = \begin{bmatrix} \dfrac{-jL_2}{\left(-M^2+L_1L_2\right)\omega} & \dfrac{jM}{\left(-M^2+L_1L_2\right)\omega} \\ \dfrac{jM}{\left(-M^2+L_1L_2\right)\omega} & \dfrac{-jL_1}{\left(-M^2+L_1L_2\right)\omega} \end{bmatrix} \quad (1)$$

where $L_1$ and $L_2$ are the inductors of the first and second oscillator and $M = k\cdot(L_1L_2)^{1/2}$ is the coupling inductance. The

oscillators are described by their admittance functions $Y_{T1}(V,\omega)$ and $Y_{T1}(V,\omega)$, where $V$ and $\omega$ are the excitation amplitude and frequency. These functions are extracted through a HB analysis of each oscillator in standalone operation [Fig. 1(a)] using an auxiliary generator (AG) [7], so $Y_{Ti}$, where $i = 1, 2$, is the ratio between the AG current and voltage. One has $Y_{Ti} = 0$ in free-running conditions. When coupled, and noting $y_{12} = y_{12}$ in (1) the two-oscillator system is governed by:

$$\begin{aligned}\left[Y_{T1}(V_1,\omega)+j/(L_1\omega)+y_{11}\right]V_1+y_{12}V_2e^{j\phi}=0\\ \left[Y_{T2}(V_1,\omega)+j/(L_2\omega)+y_{22}\right]V_2e^{j\phi}+y_{12}V_1=0\end{aligned} \quad (2)$$

where $V_1$ and $V_2$ are the oscillation amplitudes and $\phi$ the phase shift between them. The admittance $-j/(L_i\omega)$ associated with the coupled inductor in each oscillator has to be subtracted from the functions $Y_{T1}$ and $Y_{T2}$ since this inductive effect is included in (1). For two *identical* oscillators, $Y_T = Y_{T1} = Y_{T2}$, $L = L_1 = L_2$, and $y_{22} = y_{11}$, (2) simplifies to:

$$\left\{\begin{bmatrix}Y_T(V,\omega)+j/L\omega & 0\\ 0 & Y_T(V,\omega)+j/L\omega\end{bmatrix}+\begin{bmatrix}y_{11} & y_{12}\\ y_{12} & y_{11}\end{bmatrix}\right\}\begin{bmatrix}V_1\\ V_2e^{j\phi}\end{bmatrix}=0 \quad (3)$$

Because the two blocks in the left matrix are identical and the coupling matrix is circular, one will have two eigenvectors: $(V, V)^T$ and $(V,-V)^T$, where $T$ indicates transpose, so there will be two solutions with $\phi = 0°$ and $\phi = 180°$, which can be calculated from the corresponding eigenvalues [3], [6] $y_{11} - y_{12} = -j/[(L - M)\omega]$ and $y_{11} + y_{12} = -j/[(L + M)\omega]$. The respective equations are:

$$\begin{aligned}Y_T(V,\omega)+j\frac{1}{L\omega}-j\frac{1}{(L-M)\omega}=0 \quad [180°]\\ Y_T(V,\omega)+j\frac{1}{L\omega}-j\frac{1}{(L+M)\omega}=0 \quad [0°]\end{aligned} \quad (4)$$

Thus, under symmetric conditions, at least two solutions exist, with different stability properties, as shown in Section III. In the more general case of two different oscillators, to gain analytical insight one can assume weak coupling effects, as well as a small variation of a parameter $\eta$, a capacitor, for instance, in one of the oscillators. Then, (2) can be approximated as:

$$\begin{aligned}&\left[\begin{aligned}&\frac{\partial Y_{T1}}{\partial V_1}(V_1-V_{1o})+\frac{\partial Y_{T1}}{\partial\omega}'(\omega-\omega_o)+\\ &\frac{\partial Y_{T1}}{\partial\eta}(\eta-\eta_o)+j\frac{1}{L_1\omega_o}+y_{11}(\omega_o)\end{aligned}\right]V_1\\ &+\left[y_{12}(\omega_o)+\frac{\partial y_{12}}{\partial\omega}(\omega-\omega_o)\right]V_2e^{j\phi}=0\end{aligned} \quad (5)$$

$$\begin{aligned}&\left[\frac{\partial Y_{T2}}{\partial V_2}(V_2-V_{2o})+\frac{\partial Y_{T2}}{\partial\omega}'(\omega-\omega_o)+j\frac{1}{L_2\omega_o}+y_{22}(\omega_o)\right]V_2e^{j\phi}\\ &+\left[y_{12}(\omega_o)+\frac{\partial y_{12}}{\partial\omega}(\omega-\omega_o)\right]V_1=0\end{aligned}$$

where all the derivatives are calculated at the standalone free-running solution, $V_{io}$ and $\omega_{io} = \omega_{io}$, and the following quantities (evaluated at $\omega_o$) have been defined:

$$\frac{\partial Y_{T1}}{\partial\omega}'=\frac{\partial Y_{T1}}{\partial\omega}-j\frac{1}{L_1\omega^2}+\frac{\partial y_{11}}{\partial\omega},\quad \frac{\partial Y_{T2}}{\partial\omega}'=\frac{\partial Y_{T2}}{\partial\omega}-j\frac{1}{L_2\omega^2}+\frac{\partial y_{22}}{\partial\omega} \quad (6)$$

Splitting (5) into real and imaginary parts and sweeping $\phi$, one must solve a system of four equations in the unknowns $V_1, V_2$, $\omega$ and $\eta$. This analysis has been applied to two oscillators of the Van der Pol type. The two oscillators are assumed identical, except for $C_1 = C_2 + \Delta C_1$. In Fig. 2(a), the phase $\phi$ has been represented versus $\Delta C_1$. The results of the analytical formulation are compared with a HB simulation with 15 harmonics (connecting an AG to each oscillator). The excellent agreement is because $Y_{T1}$ and $Y_{T2}$ are calculated with the HB system as an inner tier [6]. For $\Delta C_1 = 0$ one obtains the even and odd modes of (4).

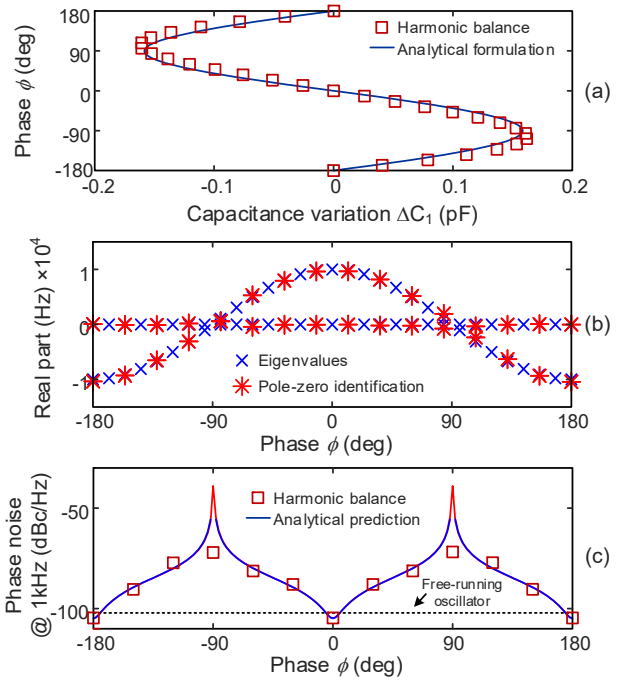


Fig. 2. Validation of the analysis method through comparison with circuit-level simulations. (a) Phase $\phi$ versus $\Delta C_1$. (b) Real part of the dominant poles. (c) Phase-noise, compared with the free-running value.

## B. *Stability analysis*

The stability relies on the introduction of a small perturbation in (2), which gives rise to the following increments: $V_i + \delta V_i(t)$, $\phi_i + \delta\phi_i(t)$, $\omega - js$, where $s$ acts like a time differentiator, applied to $(V_i + \delta V_i)\exp[j(\phi_i + \delta\phi_i)]$ [6]-[7]. Then, one obtains:

$$\begin{aligned}&\frac{\partial Y_{T1}}{\partial V_1}V_1\delta V_1+\frac{\partial Y_{T1}}{\partial\omega}'V_1(-j\frac{\delta\dot V_1}{V_1}+\delta\dot\phi_1)+\frac{\partial y_{12}}{\partial\omega}V_2e^{j\phi}(-j\frac{\delta\dot V_2}{V_2}+\delta\dot\phi_2)\\ &+\left[y_{12}(\omega_o)+\frac{\partial y_{12}}{\partial\omega}(\omega-\omega_o)\right]jV_2e^{j\phi}(-\delta\phi_1+\delta\phi_2)=0\\ &\frac{\partial Y_{T2}}{\partial V_2}V_2e^{j\phi}\delta V_2+\frac{\partial Y_{T2}}{\partial\omega}'V_2e^{j\phi}(-j\frac{\delta\dot V_2}{V_2}+\delta\dot\phi_2)+\frac{\partial y_{12}}{\partial\omega}V_1(-j\frac{\delta\dot V_1}{V_1}+\delta\dot\phi_1)\\ &+j\left[y_{12}(\omega_o)+\frac{\partial y_{12}}{\partial\omega}(\omega-\omega_o)\right]V_1(\delta\phi_1-\delta\phi_2)=0\end{aligned} \quad (7)$$

where higher order terms are neglected. Splitting (7) into real and imaginary parts, it is possible to obtain a matrix equation in terms of $\delta\bar X=\left[\delta V_1\ \delta V_2\ \delta\phi_1\ \delta\phi_2\right]^T$ and its time derivative:

$$[M_1]\delta\ddot{\bar X}=-[M_2]\delta\bar X \quad (8)$$

The terms of the two matrixes are easily gathered from the inspection of (7). The stability is determined by the eigenvalues of $[M_s] = -[M_1]^{-1}[M_2]$. Fig. 2(b) presents the variation of the real part of the dominant poles versus $\Delta C_1$. Because the whole system is autonomous, one of the eigenvalues stays at zero. Another real eigenvalue crosses through zero at each of the two turning points of the solution curve in Fig. 2(a). This result has been validated through pole-zero identification [8].

### C. Phase-noise analysis

The phase noise analysis is performed by introducing in (7) the equivalent noise-current sources $I_{N1}$ and $I_{N2}$, calculated as shown in [7]. Then, one applies the Fourier transform and multiplies by the adjoint [9]. However, this provides little insight into the phase-noise reduction mechanism. Instead, the modulation of the oscillation frequency $\delta\omega$ will be calculated here, as in [9]. This is done by setting $\delta\phi_1 = 0$, $\delta\phi = \delta\phi_2$ and neglecting $\delta V_i$:

$$\begin{aligned}
&\frac{\partial Y_{T1}}{\partial V_1} V_1 \delta V_1 + \left( \frac{\partial Y_{T1}}{\partial \omega}' V_1 + \frac{\partial y_{12}}{\partial \omega} V_2 e^{j\phi} \right) \delta\omega \\
&+ \left( y_{12}(\omega_o) + \frac{\partial y_{12}}{\partial \omega}(\omega - \omega_o) \right) j V_2 e^{j\phi} \delta\phi = I_{N1} \\
&\frac{\partial Y_{T2}}{\partial V_2} V_2 e^{j\phi} \delta V_2 + \left( \frac{\partial Y_{T2}}{\partial \omega}' V_2 e^{j\phi} + \frac{\partial y_{12}}{\partial \omega} V_1 \right) \delta\omega \\
&- \left[ y_{12}(\omega_o) + \frac{\partial y_{12}}{\partial \omega}(\omega - \omega_o) \right] j V_1 \delta\phi = I_{N2}
\end{aligned} \tag{9}$$

The phase noise is obtained by splitting (9) into real and imaginary parts and solving for $\delta\omega = j\Omega\delta\phi$, where $\Omega$ is the offset frequency. If the two oscillators are identical one obtains:

$$S(\Omega) = \left[ \sin^2(\phi + \alpha_v) + \sin^2(\phi - \alpha_v) \right] 2 |I_N|^2 (V_o^2 D\, \Omega^2)^{-1},$$

$$D = \left( \begin{array}{l} \sin(\phi + \alpha_v) \left[ \left| \frac{\partial Y_T}{\partial \omega}' \right| \sin \alpha_{v\omega T'} + \frac{\partial y_{12}}{j\partial\omega} \cos(\phi - \alpha_v) \right] - \\ \sin(\phi - \alpha_v) \left[ \left| \frac{\partial Y_T}{\partial \omega}' \right| \sin \alpha_{v\omega T'} + \frac{\partial y_{12}}{j\partial\omega} \cos(\phi + \alpha_v) \right] \end{array} \right)^2, \tag{10}$$

$$\alpha_v = ang(\partial Y_T / \partial V), \quad \alpha_{v\omega T'} = ang(\partial Y_T{}'/\partial\omega) - ang(\partial Y_T / \partial V)$$

Note that $y_{12}$ is purely imaginary. At $\phi = 0°$ and $\phi = 180°$, one has:

$$S(\Omega) = |I_N|^2 \left[ V_o^2 \left( \left| \frac{\partial Y_T}{\partial \omega}' \right| \sin \alpha_{v\omega T} + \frac{\partial y_{12}}{j\partial\omega_o} \right)^2 \Omega^2 \right]^{-1} \tag{11}$$

where:

$$\partial Y_T{}'/\partial\omega = \partial Y_T / \partial\omega - j/(L\omega_o{}^2) + \partial y_{11}/\partial\omega \tag{12}$$

The phase noise is approximately $10 \cdot \log_{10}(2)$ better than the one in free-running conditions, given by:

$$S(\Omega) = 2 |I_N|^2 / V_o^2 \left( \left| \partial Y_T / \partial\omega \right| \sin \alpha_{v\omega} \right)^2 \Omega^2 \tag{13}$$

where $\alpha_{v\omega T} = \text{ang}(\partial Y_T/\partial\omega) - \text{ang}(\partial Y_T/\partial V)$. Slight discrepancies with respect to the improvement $10 \cdot \log_{10}(2)$ would be due to the frequency derivatives of $y_{11}$ and $y_{12}$. Neglecting $\partial y_{12} / j\partial\omega$, one can write:

$$S(\Omega) = \frac{\sin^2(\phi + \alpha_v) + \sin^2(\phi - \alpha_v)}{2V_o^2 \left| \partial Y_T{}'/\partial\omega \right| \sin \alpha_{v\omega T'} \cos^2\phi \, \sin^2 \alpha_v} \frac{|I_N|^2}{\Omega^2} \tag{14}$$

The phase-shift interval ($\phi_1$, $\phi_2$) with phase noise reduction will be larger and flatter for a higher $\alpha_v$. However, this angle, which depends only on the original oscillator, affects the stability properties. Fig. 2(c) compares the predictions of (7), at the constant offset frequency $f$ = 1 kHz, with HB simulations (NH = 15) based on the conversion-matrix approach. The phase-shift interval with phase-noise reduction ($\phi_1 = 132°$, $\phi_2 = 312°$) is very small due to the small $\alpha_v$ in the Van der Pol oscillators (zero, in a describing–function analysis). Note that HB fails in the presence of two or more (practical) transistor-based oscillators. This is why the comparison with circuit-level simulations has been carried out in this simple system of two Van der Pol oscillators, where the default oscillator analysis is able to converge.

## III. Coupling at the Frequency Ratio 1/3

Injection locking through inductive coupling will also be demonstrated in the more general case of two different oscillators Osc. 1 and Osc. 2 at the frequency ratio 1/3 [Fig. 1(b)]. This will allow, for instance, reducing the phase noise of the higher frequency oscillator (Osc. 2) through the locking to Osc. 1, with a better spectral purity. Using AGs, it is possible to tune the original free-running oscillators at $\omega_o$ and $3\omega_o$.

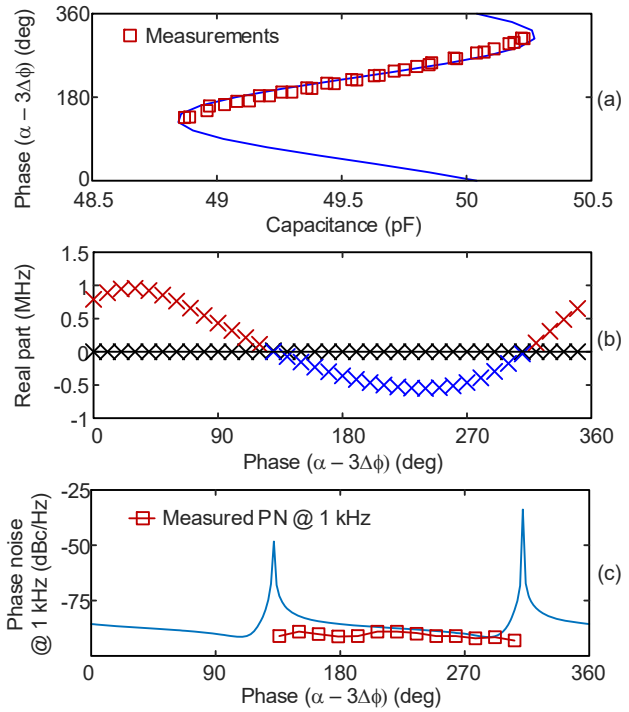


Fig. 3. Inductively-coupled oscillators at the frequency ratio 1/3. (a) Phase shift $\alpha$-3$\phi$ vs. the capacitor in Osc. 1. Measurements are superimposed. (b) Stability analysis. (c) Phase noise at $f$ = 1 kHz with measurements superimposed.

The system is formulated in terms of outer-tier admittance functions, extracted from HB. Two pairs of AGs with 180° phase shift are simultaneously introduced in Osc. 1, at $\omega_o$ and

$3\omega_o$, which provides $Y_{T1}$ and $Y_{T3}$, both depending on the amplitudes $V_1$ and $V_3$ (at the first and third harmonic terms), the excitation frequency $\omega$ and the phase shift $\phi$. The admittance function of Osc. 2, $Y_{Tb}$, is extracted with a single pair of AGs with 180º phase shift, which depends on the excitation amplitude $V_b$ and frequency. The mutual locking is mainly due to the third harmonic component, so the coupling matrix will be evaluated at $3\omega$. Neglecting the leakage at $\omega$, the system equations are:

$$\begin{aligned} Y_{T1}(V_1,V_3,\phi,\omega)&=0\\ \left(Y_{T3}(V_1,V_3,\phi,\omega)+j\frac{1}{L3\omega}+y_{11}(3\omega)\right)V_3+y_{12}(3\omega)V_b e^{j\alpha}&=0\\ \left(Y_{Tb}(V_b,\omega)+j\frac{1}{L_b 3\omega}+y_{22}(3\omega)\right)V_b e^{j\alpha}+y_{12}(3\omega)V_3&=0 \end{aligned} \quad (15)$$

where $\alpha$ is the phase shift between Osc. 2 (at $3\omega$) and that of the third harmonic component of Osc. 1. Assuming small coupling effects, the system can be linearized about the free-running solutions of the two individual oscillators:

$$\begin{aligned} &\frac{\partial Y_{T1}}{\partial V_1}\Delta V_1+\frac{\partial Y_{T1}}{\partial V_3}\Delta V_3+\frac{\partial Y_{T1}}{\partial \phi}\Delta\phi+\frac{\partial Y_{T1}}{\partial \omega}\Delta\omega+\frac{\partial Y_{T1}}{\partial \eta}\Delta\eta=0\\ &\frac{\partial Y_{T3}}{\partial V_1}V_3\Delta V_1+\frac{\partial Y_{T3}}{\partial V_3}V_3\Delta V_3+\frac{\partial Y_{T3}}{\partial \phi}V_3\Delta\phi+\frac{\partial Y_{T3}'}{\partial \omega}V_3\Delta\omega\\ &+j\frac{1}{L_1 3\omega_o}V_3+y_{11}(3\omega_o)V_3+\frac{\partial Y_{T3}}{\partial \eta}V_3\Delta\eta\\ &+\left(y_{12}(3\omega_o)+\frac{\partial y_{12}}{\partial \omega}\Delta\omega\right)V_b e^{j\alpha}=0\\ &\left(\frac{\partial Y_{Tb}}{\partial V_b}\Delta V_b+\frac{\partial Y_{Tb}'}{\partial \omega}+j\frac{1}{L_2 3\omega_o}+y_{22}(3\omega_o)\right)V_b e^{j\alpha}\\ &+y_{12}(3\omega_o)+\frac{\partial y_{12}}{\partial \omega}\Delta\omega V_3=0 \end{aligned} \quad (16)$$

where the symbol "Δ" indicates increments with respect to the free-running solution. The definitions of $\partial Y_{T3}'/\partial\omega$ and $\partial Y_{Tb}'/\partial\omega$ are analogous to those in (6). The stability and phase-noise analyses are based on the same linearization procedures described in Section II.

The method has been applied to the inductively-coupled oscillators at the frequency ratio 1/3 in Fig. 1(b). The coupling factor has been estimated from the scattering matrix of the coupled inductors as $k = 0.15$. Fig. 3(a) presents the solution curve, traced in terms of the phase shift $\alpha - 3\phi$ versus the capacitor in Osc. 1. In order to measure this, the signal from the oscillator at $\omega$ is passed through a frequency trippler, then a filter. Now, the two $3\omega$ signals can be compared in phase and the measurements are superimposed in Fig. 3(a). The stability analysis is presented in Fig. 3(b). The coupled oscillation is stable between the two turning points of the solution curve. Fig. 3(c) presents the phase noise at $f = 1$ kHz. Note that it is not possible to predict the phase noise of the system of two oscillators with the conversion matrix approach since commercial HB was not able to provide the solution with two oscillations. At the same offset, the measured phase-noise of the oscillator at 30 MHz is -87.8 dBc/Hz, so there is an improvement of about 3 dB in a significant phase-shift interval.

Fig. 4(a) and (b) present the spectra prior to the 1/3 locking and once locked. Fig. 4(c) presents the measured phase noise, obtained with an R&S® FSWP8 Phase Noise Analyzer.

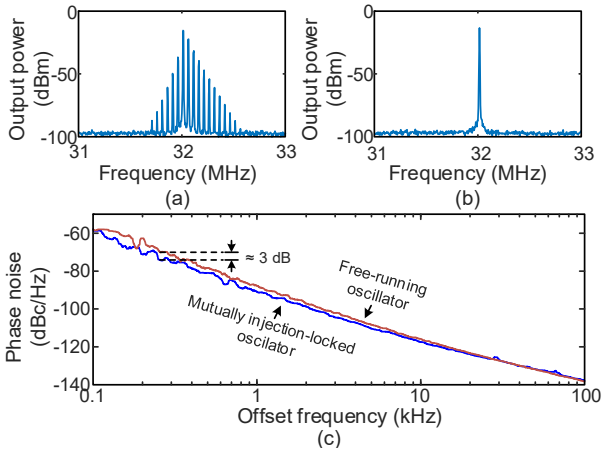


Fig. 4. Inductively-coupled oscillators at the frequency ratio 1/3 (a) Spectrum prior to the 1/3 locking and (b) once locked. (c) Measured phase noise spectra.

## IV. Conclusion

Injection locking through inductive coupling has been investigated through a formulation based on realistic models of the oscillator elements, extracted from harmonic balance simulations. It predicts the stability properties of coexisting oscillation modes and enables insight into the mechanisms for phase-noise reduction. The versatility of this kind of mutual injection locking has been demonstrated in a prototype operating at the frequency ratio 1/3.

## Acknowledgment

Work supported by the Spanish Ministry of Science and Innovation (ERDF/FEDER) TEC2017-88242-C3-1-R.

## References

[1] L. Iotti, A. Mazzanti, F. Svelto, "Insights Into Phase-Noise Scaling in Switch-Coupled Multi-Core LC VCOs for E-Band Adaptive Modulation Links," *IEEE J. Solid-State Circuits,* vol. 52, no. 7, pp. 1703-1718, 2017.

[2] J. Rimmelspacher, R. Weigel, A. Hagelauer, V. Issakov, "A Quad-Core 60 GHz Push-Push 45 nm SOI CMOS VCO with −101.7 dBc/Hz Phase Noise at 1 MHz offset, 19 % Continuous FTR and −187 dBc/Hz FoMT," *IEEE European Solid State Circuits Conf.*, Dresden, 2018, pp. 138-141.

[3] D. Murphy, H. Darabi, "A 27-GHz Quad-Core CMOS Oscillator With No Mode Ambiguity," *IEEE J. Solid-State Circuits*, vol. 53, no. 11, pp. 3208-3216, 2018.

[4] C. Sideris, P. P. Khial, A. Hajimiri, "Design and Implementation of Reference-Free Drift-Cancelling CMOS Magnetic Sensors for Biosensing Applications," *IEEE J. Solid-State Circuits,* vol. 53, pp. 3065-3075, 2018.

[5] J. Pan, A. A. Abidi, W. Jiang, D. Marković, "Simultaneous Transmission of Up To 94-mW Self-Regulated Wireless Power and Up To 5-Mb/s Reverse Data Over a Single Pair of Coils," *IEEE J. Solid-State Circuits*, vol. 54, no. 4, pp. 1003-1016, 2019.

[6] K. Kurokawa, "An Analysis of Rucker's Multidevice Symmetrical Oscillator," *IEEE Trans. Microw. Theory Techn.*, vol. 18, pp. 967-969, 1970.

[7] F. Ramírez, M. Pontón, S. Sancho, A. Suárez, "Phase−Noise Analysis of Injection−Locked Oscillators and Analog Frequency Dividers", *IEEE Trans. Microw. Theory Techn.*, vol. 56, no.2, pp. 393−407, 2008.

[8] J. Jugo, J. Portilla, A. Anakabe, A. Suarez, J. M. Collantes, "Closed-loop stability analysis of microwave amplifiers," *Electronics Letters*, vol. 37, no. 4, Mar, 2001, pp. 226-228.

[9] V. Rizzoli, F. Mastri, and D. Masotti, "General noise analysis of nonlinear microwave circuits by the piecewise harmonic-balance technique," *IEEE Trans. Microw. Theory Techn.*, vol. 42, no. 5, pp. 807–819, May 1994.